Delay Compensation for Distributed MIMO Radar With Non-Orthogonal Waveforms

Cengcang Zeng, Fangzhou Wang, *Student Member, IEEE*, Hongbin Li, *Fellow, IEEE*, and Mark A. Govoni, *Senior Member, IEEE*

***Abstract*—Distributed multi-input multi-output (MIMO) radar with non-orthogonal waveforms has become a critical problem because waveform orthogonality may be lost as waveforms experience distinct delays and Doppler across different transmit-receive propagation paths. In such cases, the widely used matched filter (MF) cannot perfectly separate the waveforms, and it outputs the filtered echo of the desired waveform (auto term) as well as multiple undesired waveform residuals (cross terms). In this paper, a transmit delay compensation scheme is proposed by employing a set of transmit delay compensation variables to control the cross terms so that they can be utilized to enhance target detection. Specifically, the probability of detection is maximized by optimizing the delay parameters. To solve the resulting nonconvex problem, an optimum solution based on multi-dimensional search and a computationally efficient suboptimal method are proposed. Simulation results show that the proposed delay compensation approach can substantially improve the target detection performance.**

***Index Terms*—Distributed MIMO radar, probability of detection, transmit delay compensation, non-orthogonal waveforms.**

I. Introduction

In RECENT years, distributed multi-input multi-output (MIMO) radar, an architecture that employs widely separated antennas to form the transmit and receive apertures, has received significant attention [1]–[4]. Widely separated antennas allows one to capture the spatial diversity of the target's radar cross section (RCS), which can be employed to enhance target detection [5]. Among extensive MIMO radar related studies, some recent works considered system optimization via space-time code design [6], antenna placement [7], power allocation [8], waveform design [9], and joint transmit and receive design [10], [11]. The exploitation of signal/clutter structures for target detection was investigated in [12]–[17]. In addition, [18] and [19] examined the synchronization effect on target localization, and respectively, signal detection in MIMO radar. Meanwhile, [20] derived the Cramer-Rao bound for MIMO radar target localization with phase errors, while the exploitation of signal sparsity was investigated in [21], [22].

Most existing MIMO radar works assume the transmitters (TXs) emit multiple orthogonal probing waveforms with zero cross-correlation, which are separated by a set of matched filters (MFs) at the receivers (RXs). Assuming the waveforms are orthogonal and thus perfectly separable at the RXs, only the filtered echo of the desired waveform (*auto term*) is present at each MF output, but not the undesired waveform residuals (*cross terms*). However, in practice, maintaining waveform orthogonality at the RXs across all time delays and Doppler frequencies is impossible [23]. The effects of cross terms induced by non-orthogonal waveforms were examined in [24]–[27] for direction-of-arrival (DOA) estimation and in [28]–[30] for target detection. These studies model the cross terms as either deterministic [28], [29] or random quantities with some covariance matrices [24], [25], [30].

Interestingly, it was shown in [28] that the waveform cross terms may behave as friend or foe in target detection, depending on how the cross terms are added with the auto terms, which is affected by the phase, delay, and frequency offsets among different TX-RX propagation paths. In order to benefit from cross terms for target detection, we propose herein a transmit delay compensation scheme that tries to align the cross and auto terms at the MF outputs. Specifically, we introduce a set of transmit delay compensation variables at the TXs to control the amplitude and phase of cross terms so that they can add with the auto terms constructively. The design criterion is based on maximizing the probability of detection with respect to (w.r.t.) the delay compensation variables. The resulting nonconvex problem is solved through both an optimum method based on multi-dimensional search and a computationally efficient suboptimal algorithm. Our numerical results show that the proposed delay compensation scheme significantly outperforms the conventional approach without delay compensation when the MIMO waveforms are non-orthogonal or are not perfectly separated at the RXs.

II. Signal Model

We consider a distributed MIMO radar consisting of M widely separated transmit antennas (TXs) and N receive antennas (RXs) with M non-orthogonal waveforms. The waveforms may arrive at the RXs asynchronously since the distances associated with different TX-RX propagation paths are different. At the TXs, pulsed transmission is employed to help determine if there is a moving target in an area of interest. During a coherent processing interval (CPI), each TX emits a succession

Manuscript received September 2, 2021; revised October 23, 2021; accepted October 24, 2021. Date of publication October 27, 2021; date of current version January 20, 2022. This work was supported in part by the Army Research Office under Cooperative Grant W911NF-19-2-0234 and in part by the National Science Foundation under Grant ECCS-1923739. The associate editor coordinating the review of this manuscript and approving it for publication was Dr. Jean Pierre Delmas. *(Corresponding author: Hongbin Li.)*

Cengcang Zeng, Fangzhou Wang, and Hongbin Li are with the Department of Electrical and Computer Engineering, Stevens Institute of Technology, Hoboken, NJ 07030 USA (e-mail: czeng2@stevens.edu; fwang11@stevens.edu; hli@stevens.edu).

Mark A. Govoni is with the Army Research Laboratory, Aberdeen Proving Ground, Aberdeen, MD 21005 USA (e-mail: mgovoni@ieee.org).

Digital Object Identifier 10.1109/LSP.2021.3123582

of K pulses. At the RX, the received signal is down-converted, matched-filtered, and sampled at the pulse rate. The $K \times 1$ noise-free output at the n-th RX, matched to the m-th waveform, can be expressed as [28]:

$$\widetilde{\mathbf{x}}_{mn} = \alpha \mathbf{S}_n \widetilde{\boldsymbol{\mathcal{X}}}_{mn} \widetilde{\mathbf{h}}_{mn}, m = 1, \ldots, M, n = 1, \ldots, N, \quad (1)$$

where α denotes the target amplitude, $\mathbf{S}_n \in \mathbb{C}^{K \times M}$ the Doppler steering matrix, $\widetilde{\chi}_{mn} \in \mathbb{C}^{M \times M}$ the diagonal ambiguity function matrix, and $\widetilde{\mathbf{h}}_{mn} \in \mathbb{C}^{M \times 1}$ the channel vector. Specifically, $\mathbf{S}_n$, $\widetilde{\chi}_{mn}$, and $\widetilde{\mathbf{h}}_{mn}$ are given by [28]

$$\mathbf{S}_n = [\mathbf{s}(f_{1n}), \ldots, \mathbf{s}(f_{Mn})], \quad (2)$$

$$[\widetilde{\boldsymbol{\mathcal{X}}}_{mn}]_{\bar{m}\bar{m}} = \chi_{m\bar{m}}(\tau_{mn} - \tau_{\bar{m}n}, f_{\bar{m}n} - f_{mn}), \quad (3)$$

$$[\widetilde{\mathbf{h}}_{mn}]_{\bar{m}} = \xi_{\bar{m}n} e^{-\jmath 2\pi f_c \tau_{\bar{m}n}} e^{\jmath 2\pi f_{mn}(\tau_{mn} - \tau_{\bar{m}n})}, \quad (4)$$

where

- f_{mn} denotes the normalized target Doppler frequency, $\mathbf{s}(f_{mn}) \in \mathbb{C}^{K \times 1}$ the Doppler steering vector at f_{mn}, and f_c the carrier frequency.
- ξ_{mn} and τ_{mn} are the pathloss (nonnegative) channel coefficient and propagation delay, respectively.
- $\chi_{m\bar{m}}(\mu, f) = \int q_m(\nu) q^*_{\bar{m}}(\nu - \mu) e^{\jmath 2\pi f \nu} d\nu$ denotes the *cross ambiguity function* (CAF) between two different radar waveforms $q_m(t)$ and $q_{\bar{m}}(t)$.

Note that the diagonal ambiguity function matrix $\widetilde{\chi}_{mn}$ in (3) consists of M components, i.e., one auto term ($m = \bar{m}$) and $M - 1$ cross terms ($m \neq \bar{m}$). To see this, consider the case when $M = 3$ and $N = 1$. The RX implements 3 matched filters (MFs), each matched to one transmitted waveform. The output of the first MF matched to the first (desired) waveform is given by [cf. (1) for $m = 1$ and $n = 1$]:

$$\begin{aligned}\widetilde{\mathbf{x}}_{11} = {} & \alpha [\widetilde{\boldsymbol{\mathcal{X}}}_{11}]_{11} [\widetilde{\mathbf{h}}_{11}]_1 \mathbf{s}(f_{11}) + \alpha [\widetilde{\boldsymbol{\mathcal{X}}}_{11}]_{22} [\widetilde{\mathbf{h}}_{11}]_2 \mathbf{s}(f_{21}) \\ & + \alpha [\widetilde{\boldsymbol{\mathcal{X}}}_{11}]_{33} [\widetilde{\mathbf{h}}_{11}]_3 \mathbf{s}(f_{31}), \end{aligned} \quad (5)$$

where the first term is the auto term from the desired waveform, and the second and third are the cross terms from the other two undesired waveforms. It was shown in [28] that the cross terms may benefit or harm the radar performance, depending on how they interact with the auto term. The problem of interest for this work is to introduce and design suitable transmit delay parameters to exploit cross terms for target detection.

III. Proposed Approach

In this section, we first introduce transmit delays to the signal model in (1). Then, a design criterion based on the probability of detection of an energy detector is presented, followed by our proposed solutions. It is noted that the proposed scheme requires the knowledge of the location or delay associated with the target, which is available when the radar operates in a tracking mode.

A. Transmit Delay Compensation

The additive relation shown in (1) and (3) shows that the propagation delays τ_{mn} associated with different TX-RX paths affect if the auto and cross terms add constructively or destructively. Thus, we can introduce an additional delay Δ_m for each TX so that the cross terms at the MF output can add up constructively. Since only the relative propagation delay among different TX-RX paths matters, without loss of generality, we let the first TX be the reference, i.e., $\Delta_1 = 0$. Then, the problem is to design the rest $M - 1$ delay variables, $\{\Delta_m\}_{m=2}^M$.

For notational distinction, $\widetilde{\chi}_{mn}$ and $\widetilde{\mathbf{h}}_{mn}$ in (1) are now represented by χ_{mn} and $\mathbf{h}_{mn}$ to signify the use of the delay compensation at the TXs:

$$[\boldsymbol{\mathcal{X}}_{mn}]_{\bar{m}\bar{m}} = \chi_{m\bar{m}}(\tau_{mn} + \Delta_m - \tau_{\bar{m}n} - \Delta_{\bar{m}}, f_{\bar{m}n} - f_{mn}), \quad (6)$$

$$[\mathbf{h}_{mn}]_{\bar{m}} = \xi_{\bar{m}n} e^{-\jmath 2\pi \hat{f}_c(\tau_{\bar{m}n} + \Delta_{\bar{m}})} e^{\jmath 2\pi f_{mn}(\tau_{mn} + \Delta_m - \tau_{\bar{m}n} - \Delta_{\bar{m}})}. \quad (7)$$

In turn, the noise-free received signal in (1) is now written as

$$\mathbf{x}_{mn}(\Delta_m) = \alpha \mathbf{S}_n \boldsymbol{\mathcal{X}}_{mn} \mathbf{h}_{mn}, \quad (8)$$

where the k-th element of $\mathbf{x}_{mn}(\Delta_m)$ can be expressed as [28]

$$\begin{aligned} \mathbf{x}_{mn}(k, \Delta_m) = {} & \alpha \xi_{mn} e^{\jmath 2\pi k T_s f_{mn}} \chi_{mm}(0, 0) \\ & \times e^{-\jmath 2\pi f_c(\tau_{mn} + \Delta_m)} + \sum_{\bar{m} \neq m} \alpha \xi_{\bar{m}n} e^{\jmath 2\pi k T_s f_{\bar{m}n}} \\ & \times \chi_{m\bar{m}}(\tau_{mn} + \Delta_m - \tau_{\bar{m}n} - \Delta_{\bar{m}}, f_{\bar{m}n} - f_{mn}) \\ & \times e^{-\jmath 2\pi f_c(\tau_{\bar{m}n} + \Delta_{\bar{m}})} e^{\jmath 2\pi f_{mn}(\tau_{mn} + \Delta_m - \tau_{\bar{m}n} - \Delta_{\bar{m}})}, \\ k = {} & 0, \ldots, K - 1. \end{aligned} \quad (9)$$

Similar to (5), the second term (expressed in a sum) represents the $M - 1$ cross terms.

To optimize the transmit delays Δ_m, we consider maximizing the probability of detection of an energy detector. Specifically, the problem of detecting a target can be formulated as the following binary hypothesis testing problem:

$$\begin{aligned} & \mathcal{H}_0 : \mathbf{y}_{mn} = \mathbf{w}_{mn}, \\ & \mathcal{H}_1 : \mathbf{y}_{mn} = \mathbf{x}_{mn}(\Delta_m) + \mathbf{w}_{mn}, \\ & \qquad m = 1, 2, \ldots, M, \ n = 1, 2, \ldots, N, \end{aligned} \quad (10)$$

where $\mathbf{w}_{mn}$ is the noise. A simple solution to the above hypothesis testing is the energy detector that non-coherently integrates the MF output energy [1]:

$$T \triangleq \sum_{n=1}^{N} \sum_{m=1}^{M} \mathbf{y}_{mn}^H \mathbf{y}_{mn} \underset{\mathcal{H}_0}{\overset{\mathcal{H}_1}{\gtrless}} \gamma, \quad (11)$$

where γ denotes the threshold. The probability of false alarm and the probability of detection with a non-fluctuating target for the above detector are given by [28]

$$P_f = \frac{\Gamma(KMN) - \bar{\Gamma}(KMN, \gamma/\sigma^2)}{\Gamma(KMN)}, \quad (12)$$

$$P_d = Q_{KMN}\left(\sqrt{\lambda}, \sqrt{\frac{2\gamma}{\sigma^2}}\right), \quad (13)$$

where $\Gamma(\cdot)$ and $\bar{\Gamma}(\cdot, \cdot)$ denote the Gamma[31, p.255] the upper incomplete Gamma functions[31, p.260], respectively. $Q_m(a, b)$ is the generalized Marcum-Q function[32, p.5]and λ is the noncentrality parameter, which takes the following form:

$$\lambda = \sum_{m=1}^{M} \sum_{n=1}^{N} \frac{2}{\sigma^2} \|\mathbf{x}_{mn}(\Delta_m)\|^2. \quad (14)$$

Following the monotonicity of the generalized Marcum function, maximizing the probability of detection is equivalent to maximizing the noncentrality parameter λ. Thus, our transmit delay design problem can be formulated as:

$$\max_{\{\Delta_m\}_{m=2}^M} \quad \sum_{m=1}^{M}\sum_{n=1}^{N} \|\mathbf{x}_{mn}(\Delta_m)\|^2. \tag{15}$$

B. Solutions

A direct way to solve (15) is to employ multi-dimensional search over the parameter space. Specifically, we can enumerate all possible solutions on a discretized search grid and find the optimum one for the problem. However, this is doable only when M is small. The associated computational complexity grows exponentially with M. To address this issue, we need find an alternative suboptimal solution.

There are two factors that affect the impact of cross terms on detection, namely their magnitudes and phases relative to the phase of the auto term. In general, the magnitudes should be made as large as possible, so that they can contribute more to the MF output energy; on the other hand, their phases should be made as close as possible to the phase of the auto term, so that they can add up constructively. However, it is impossible to simultaneously meet these requirements due to limited design parameters (i.e., $M-1$ delays). Our strategy is to focus on the dominant cross terms associated with the strongest channels, i.e., the channels associated with the TX that has the shortest TX-target distances.[1] Without loss of generality, suppose the strongest channels are associated with $m=1$, i.e., the first TX. Then, we can approximate the cost function in (15) by focusing on the cross term generated by the 1st TX and neglect the effects of the others. Although the approximation is based on the presence of a dominant channel, numerical results show that this approach works well even if no dominant channel exists.

Base on the above discussion, we can obtain an approximate solution to problem (15) by:

$$\max_{\{\Delta_m\}_{m=2}^M} \quad \sum_{m=1}^{M}\sum_{n=1}^{N} \|\mathbf{z}_{mn}(\Delta_m)\|^2, \tag{16}$$

where the k-th element of $\mathbf{z}_{mn}(\Delta_m)$ is

$$\begin{aligned}\mathbf{z}_{mn}(k,\Delta_m) &= \alpha\xi_{mn}e^{\jmath 2\pi k T_s f_{mn}}\chi_{mm}(0,0)e^{-\jmath 2\pi f_c(\tau_{mn}+\Delta_m)}\\ &+ \alpha\xi_{1n}e^{\jmath 2\pi k T_s f_{1n}}\chi_{m1}(\tau_{mn}+\Delta_m-\tau_{2n}, f_{1n}-f_{mn})\\ &\times e^{-\jmath 2\pi f_c(\tau_{1n})}e^{\jmath 2\pi f_{mn}(\tau_{mn}+\Delta_m-\tau_{1n})}, k=0,\ldots,K-1,\end{aligned} \tag{17}$$

which is obtained by keeping only the auto term associated with TXm (channel ξ_{mn}) and the dominant cross term associated with channel ξ_{1n} in (9). It can be observed from (17) that the m-th MF output is affected by only the m-th delay Δ_m. Thus, the optimization problem in (16) can be decomposed into $M-1$ independent subproblems:

$$\max_{\Delta_m} \quad \|\mathbf{z}_{mn}(\Delta_m)\|^2, m=2,\ldots,M. \tag{18}$$

Note that problem (18) can be solved through $(M-1)$ independent one-dimensional searches.

[1]Note that for a given RX, the waveforms arrive at the RX with the same target-RX path but different TX-target paths. So the dominant channel is associated with the TX with the shortest TX-target distance.

Algorithm 1: Proposed Suboptimal Solution for the Design Problem in (15).

Input: Waveform CAFs and ξ_{mn}.
Output: Delay compensation parameters $\{\Delta_m\}_{m=2}^M$
For $m=2,\ldots,M$ **do**
1) Find the initial delay compensations $\hat{\Delta}_m$ by using (20)
2) Use (21) to obtain an updated delay compensation Δ_m with phase alignment via local search
end
Return: Delay compensation Δ_m.

We next discuss how to further improve the efficiency via a 2-step search approach. Note that without any prior knowledge about the range of Δ_m, the one-dimensional search can still be time consuming. We can lower the complexity by exploiting further insight into (17) to reduce the search interval and complexity. Specifically, it can be observed from (17) that the delay Δ_m affects not only the relative phase between the auto and cross terms, but also magnitude of the CAF χ_{m1}. Note that the CAF χ_{m1} is complex-valued and can be expressed in magnitude and phase:

$$\chi_{m1} = |\chi_{m1}|e^{j\theta_{m1}}. \tag{19}$$

Its magnitude $|\chi_{m1}|$ should be made as large as possible to maximize its contribution to the received energy. Therefore, we can determine an initial estimate of the delay by maximizing the CAF:

$$\begin{aligned}\hat{\Delta}_m = \ &\arg\max_{\Delta_m} |\chi_{m1}(\tau_{mn}+\Delta_m-\tau_{1n}, f_{1n}-f_{mn})|,\\ &m=2,\ldots,M.\end{aligned} \tag{20}$$

Then, we can search in a small interval centered around $\hat{\Delta}_m$ so that the phase difference between the auto and cross terms are minimized. It is easy to see from (17) that the phase difference can be expressed as (neglecting delay-independent constants)

$$\begin{aligned}\Theta_{m1} = \ &-2\pi f_c(\tau_{mn}+\Delta_m-\tau_{1n})\\ &-\theta_{m1}(\Delta_m)-2\pi f_{mn}(\tau_{mn}+\Delta_m-\tau_{1n}).\end{aligned} \tag{21}$$

which, with 2π-phase wrapping, has a periodic pattern. It is sufficient to cover one 2π-period of the phase difference, by varying Δ_m within the range of $[\hat{\Delta}_m - 1/f_c, \hat{\Delta}_m + 1/f_c]$. As shown in [33], the magnitude $|\chi_{m1}|$ varies much slower with respect to (w.r.t.) the delay than the phase θ_{m1}. Therefore, we only need search over a small interval around the initial delay estimate $\hat{\Delta}_m$ to achieve phase alignment, without affecting the magnitude. A summary of the proposed approach is presented in **Algorithm 1**.

IV. Simulation Results

In this section, numerical simulations are provided to demonstrate the performance of the proposed transmit delay compensation scheme by evaluating the probability of detection with the energy detector (11). The delay variables are computed either by (15), which is referred to as the *optimal* method, or (18), which is referred to as the *suboptimal* method. We compare these delay compensation methods with the conventional scheme with *no compensation*.

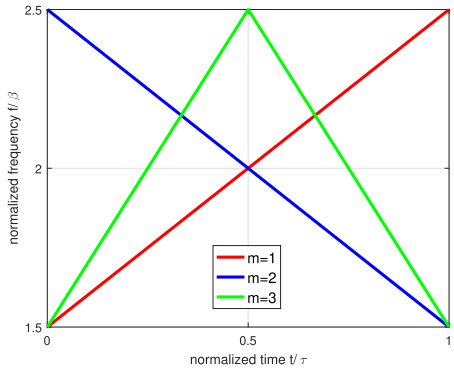

Fig. 1. The instantaneous frequency of the chirp waveforms.

In the simulation, two distributed MIMO radar configurations with $M = 2$ or $M = 3$ are considered. We fix $N = 1$ RX for both cases, since transmit compensation only affects the TX-target propagation delay and is independent of the number of RXs. However, the value of M does have an impact. Note that with $M = 2$ TXs, the suboptimal (18) is identical to the optimal (15) since there is only one cross term in the MF output and no approximation is involved. Meanwhile, for $M = 3$, there are more than one cross terms in the MF output, (18) yields only an approximate solution. Since the approximation assumes the presence of a dominant channel, we consider two scenarios. The first scenario contains a dominant channel, whereas the channels of the second scenario have identical strength. In the latter case, we randomly pick a channel and its associated cross term for alignment. It turns out, as shown next, the compensation can still lead to significant performance gain.

The signal-to-noise ratio (SNR) of the (m, n)-th TX-RX pair is defined as

$$\text{SNR}_{mn} = \frac{|\xi_{mn}|^2 \mathbb{E}\{|\alpha|^2\}}{\sigma_{mn}^2}, \tag{22}$$

where σ_{mn}^2 is the noise variance and set to 1. In addition, a Swerling I target model is considered with $\alpha \sim \mathcal{CN}(0, \sigma^2)$ being randomly generated in the simulation trials. Other simulation parameters are set as follows: the probability of false alarm is $P_f = 10^{-4}$ and $N = 1$.

Linear frequency modulation waveforms $q_m(t)$ with overlapping instantaneous frequency are employed for testing [33]:

$$q_1(t) = \frac{1}{\sqrt{\tau}} e^{\jmath(\pi\beta t^2/\tau + 3\pi\beta t)}, \; 0 \le t < \tau, \tag{23}$$

$$q_2(t) = \frac{1}{\sqrt{\tau}} e^{\jmath(-\pi\beta t^2/\tau + 5\pi\beta t)}, \; 0 \le t \le \tau, \tag{24}$$

$$q_3(t) = \begin{cases} \frac{1}{\sqrt{\tau}} e^{\jmath(2\pi\beta t^2/\tau + 3\pi\beta t)}, & 0 \le t < \frac{\tau}{2}, \\ \frac{1}{\sqrt{\tau}} e^{\jmath(-2\pi\beta t^2/\tau + 7\pi\beta t)}, & \frac{\tau}{2} \le t \le \tau, \end{cases} \tag{25}$$

where τ and β denote the duration and bandwdith, respectively, of the chirps. The instantaneous frequency of of the chirps is displayed in Fig. 1. For the case of $M = 2$, only the first two waveforms are employed.

Fig. 2 shows the performance when $M = 3$, where the probability of detection is obtained by the two compensation schemes as well as the no compensation one. In Fig. 2(a), the channels are $\xi_{11} = 10\xi_{21} = 10\xi_{31}$, i.e., channel 11 associated with TX 1

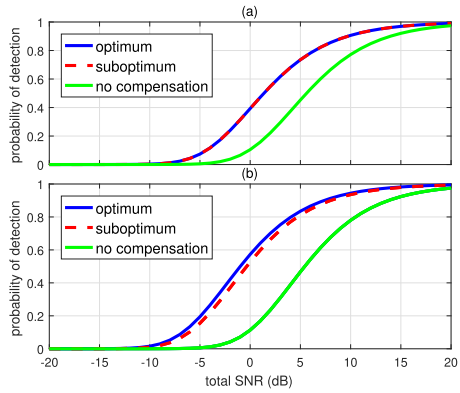

Fig. 2. Probability of detection versus the total SNR for the energy detector when $M = 3$: (a) $\xi_{11} = 10\xi_{21} = 10\xi_{31}$; (b) $\xi_{11} = \xi_{21} = \xi_{31}$.

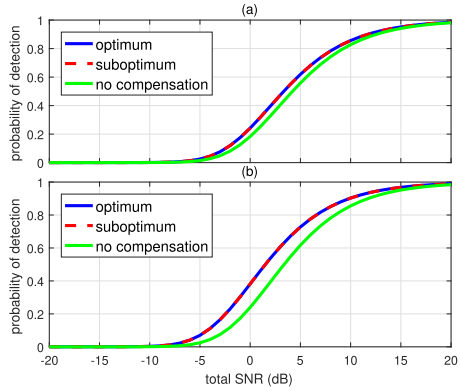

Fig. 3. Probability of detection versus the total SNR for the energy detector when $M = 2$: (a) $\xi_{11} = 10\xi_{21}$; (b) $\xi_{11} = \xi_{21}$.

is the dominant channel. It is seen that the suboptimal scheme is identical to the optimal method. On the other hand, in Fig. 2(b), we set $\xi_{11} = \xi_{21} = \xi_{31}$, in which case no dominant channel exists. It is interesting to see that the suboptimal method exhibits only a small performance loss relative to the optimal one. Both results show that the proposed delay compensation schemes significantly outperform the conventional approach with no compensation.

The counterpart results for $M = 2$ are displayed in Figs. 3(a) and 3(b). As expected, the suboptimal compensation method is identical to the optimal one. It is observed that the delay compensation yields less performance benefit over the conventional approach with no compensation, in particular when a dominant channel is present. This is due to the reduced diversity, as the weaker channel contributes less to the diversity gain.

V. Conclusion

A transmit delay compensation approach was proposed for distributed MIMO radar with non-orthogonal waveforms. The approach aims to maximize the probability of detection w.r.t. the delay parameters. The resulting optimization problem was solved via both an optimal method based on nonlinear research as well as a suboptimal two-step method. It was shown that our delay compensation solutions can achieve improved detection performance over the conventional approach with no compensation in distributed MIMO radar.

REFERENCES

[1] A. M. Haimovich, R. S. Blum, and L. J. Cimini, "MIMO radar with widely separated antennas," *IEEE Signal Process. Mag.*, vol. 25, no. 1, pp. 116–129, Jan. 2008.

[2] P. Wang, H. Li, and B. Himed, "Moving target detection using distributed MIMO radar in clutter with nonhomogeneous power," *IEEE Trans. Signal Process.*, vol. 59, no. 10, pp. 4809–4820, Oct. 2011.

[3] Q. He, R. S. Blum, H. Godrich, and A. M. Haimovich, "Target velocity estimation and antenna placement for MIMO radar with widely separated antennas," *IEEE J. Sel. Topics Signal Process.*, vol. 4, no. 1, pp. 79–100, Feb. 2010.

[4] W. Liu, J. Liu, C. Hao, Y. Gao, and Y.-L. Wang, "Multichannel adaptive signal detection: Basic theory and literature review," *Sci. China Inf. Sci.*, Feb. 2021, doi: 10.1007/s11432-020-3211-8.

[5] E. Fishler, A. Haimovich, R. S. Blum, L. J. Cimini, D. Chizhik, and R. A. Valenzuela, "Spatial diversity in radars-models and detection performance," *IEEE Trans. Signal Process.*, vol. 54, no. 3, pp. 823–838, Mar. 2006.

[6] X. Zhang, F. Wang, and H. Li, "Multi-aperture space-time transmit and receive design for MIMO radar," *IEEE Signal Process. Lett.*, vol. 28, pp. 947–951, 2021.

[7] Y. Yang *et al.*, "Fast optimal antenna placement for distributed MIMO radar with surveillance performance," *IEEE Signal Process. Lett.*, vol. 22, no. 11, pp. 1955–1959, Nov. 2015.

[8] H. Zhang, W. Liu, Z. Zhang, W. Lu, and J. Xie, "Joint target assignment and power allocation in multiple distributed MIMO radar networks," *IEEE Syst. J.*, vol. 15, no. 1, pp. 694–704, Mar. 2021.

[9] X. Yu, K. Alhujaili, G. Cui, and V. Monga, "MIMO radar waveform design in the presence of multiple targets and practical constraints," *IEEE Trans. Signal Process.*, vol. 68, pp. 1974–1989, 2020.

[10] J. Li, G. Liao, Y. Huang, Z. Zhang, and A. Nehorai, "Riemannian geometric optimization methods for joint design of transmit sequence and receive filter on MIMO radar," *IEEE Trans. Signal Process.*, vol. 68, pp. 5602–5616, 2020.

[11] L. Lan, G. Liao, J. Xu, Y. Zhang, and B. Liao, "Transceive beamforming with accurate nulling in FDA-MIMO radar for imaging," *IEEE Trans. Geosci. Remote Sens.*, vol. 58, no. 6, pp. 4145–4159, Jun. 2020.

[12] L. Pan, Y. Gao, and Z. Xin, "Subspace signal detection using distributed mimo radar in structured interference and Gaussian disturbance," in *Proc. Int. Conf. Control, Automat. Inf. Sci.*, 2019, pp. 1–5.

[13] J. Liu and J. Li, "Robust detection in MIMO radar with steering vector mismatches," *IEEE Trans. Signal Process.*, vol. 67, no. 20, pp. 5270–5280, Oct. 2019.

[14] J. Liu, W. Liu, J. Han, B. Tang, Y. Zhao, and H. Yang, "Persymmetric GLRT detection in MIMO radar," *IEEE Trans. Veh. Technol.*, vol. 67, no. 12, pp. 11 913–11923, Dec. 2018.

[15] W. Liu, Y. Wang, J. Liu, W. Xie, H. Chen, and W. Gu, "Adaptive detection without training data in colocated MIMO radar," *IEEE Trans. Aerosp. Electron. Syst.*, vol. 51, no. 3, pp. 2469–2479, Jul. 2015.

[16] J. Liu, S. Zhou, W. Liu, J. Zheng, H. Liu, and J. Li, "Tunable adaptive detection in colocated MIMO radar," *IEEE Trans. Signal Process.*, vol. 66, no. 4, pp. 1080–1092, Feb. 2018.

[17] S. Yan, C. Hao, M. Liu, and D. Chen, "Bistatic MIMO sonar space-time adaptive processing based on knowledge-aided transform," in *Proc. MTS/IEEE Kobe Techno-Oceans Conf. (OTO)*, 2018, pp. 1–5.

[18] H. Song, G. Wen, Y. Liang, L. Zhu, and D. Luo, "Target localization and clock refinement in distributed MIMO radar systems with time synchronization errors," *IEEE Trans. Signal Process.*, vol. 69, pp. 3088–3103, 2021.

[19] Q. Hu, H. Su, S. Zhou, Z. Liu, and J. Liu, "Target detection in distributed mimo radar with registration errors," *IEEE Trans. Aerosp. Electron. Syst.*, vol. 52, no. 1, pp. 438–450, Feb. 2016.

[20] Q. He and R. S. Blum, "Cramer-Rao bound for MIMO radar target localization with phase errors," *IEEE Signal Process. Lett.*, vol. 17, no. 1, pp. 83–86, Jan. 2010.

[21] P. Chen, Z. Cao, Z. Chen, and X. Wang, "Off-grid DOA estimation using sparse Bayesian learning in MIMO radar with unknown mutual coupling," *IEEE Trans. Signal Process.*, vol. 67, no. 1, pp. 208–220, Jan. 2019.

[22] W. Shi, J. Huang, Q. Zhang, and J. Zheng, "DOA estimation in monostatic MIMO array based on sparse signal reconstruction," in *Proc. IEEE Int. Conf. Signal Process., Commun. Comput.*, 2016, pp. 1–4.

[23] Y. I. Abramovich and G. J. Frazer, "Bounds on the volume and height distributions for the MIMO radar ambiguity function," *IEEE Signal Process. Lett.*, vol. 15, pp. 505–508, 2008.

[24] C. Mao, F. Wen, Z. Zhang, and Z. Gong, "New approach for DOA estimation in MIMO radar with nonorthogonal waveforms," *IEEE Sens. Lett.*, vol. 3, no. 7, pp. 1–4, Jul. 2019.

[25] C. Shen, F. Dong, F. Wen, Z. Gong, and K. Zhang, "An improved propagator estimator for DOA estimation in monostatic MIMO radar in the presence of imperfect waveforms," *IEEE Access*, vol. 7, pp. 148 148771–148 778, 2019.

[26] B. Liao, "Fast angle estimation for MIMO radar with nonorthogonal waveforms," *IEEE Trans. Aerosp. Electron. Syst.*, vol. 54, no. 4, pp. 2091–2096, Aug. 2018.

[27] F. Wen, "Computationally efficient DOA estimation algorithm for MIMO radar with imperfect waveforms," *IEEE Commun. Lett.*, vol. 23, no. 6, pp. 1037–1040, Jun. 2019.

[28] H. Li, F. Wang, C. Zeng, and M. A. Govoni, "Signal detection in distributed MIMO radar with non-orthogonal waveforms and sync errors," *IEEE Trans. Signal Process.*, vol. 69, pp. 3671–3684, 2021.

[29] M. Akçakaya and A. Nehorai, "MIMO radar sensitivity analysis for target detection," *IEEE Trans. Signal Process.*, vol. 59, no. 7, pp. 3241–3250, Jul. 2011.

[30] P. Wang and H. Li, "Target detection with imperfect waveform separation in distributed MIMO radar," *IEEE Trans. Signal Process.*, vol. 68, pp. 793–807, 2020.

[31] M. Abramowitz and I. A. Stegun, *Handbook of Mathematical Functions With Formulas, Graphs, and Mathematical Tables*. New York, NY, USA: Dover, 1972.

[32] J. Marcum, "A statistical theory of target detection by pulsed radar," *IRE Trans. Inf. Theory*, vol. 6, no. 2, pp. 59–267, 1960.

[33] F. Wang, C. Zeng, H. Li, and M. A. Govoni, "Detection performance of distributed MIMO radar with asynchronous propagation and timing/phase errors," in *Proc. IEEE Int. Radar Conf.*, 2020, pp. 13–18.